

## Optimization of sponge iron (direct reduced iron) production with Box-Wilson experimental design by using iron pellets and lignite as reductant

İbrahim Sönmez<sup>a,\*</sup>, Kemal Şahbudak<sup>b</sup>

<sup>a</sup> Metallurgical and Materials Engineering Department, Hitit University, Çorum, 19030, Türkiye

<sup>b</sup> Metallurgical and Materials Engineering Department, Sivas Cumhuriyet University, Sivas, 58140, Türkiye

(\*Corresponding author: [ibrahimsonmez@hitit.edu.tr](mailto:ibrahimsonmez@hitit.edu.tr))

Submitted: 7 June 2022; Accepted: 30 May 2023; Available On-line: 31 October 2023

**ABSTRACT:** Turkey's iron ores may be used to manufacture sponge iron, and the country's coal resources, which are plentiful despite being of poor quality, can be used as a reducing agent. With such a production, Electric Arc Furnace based on scrap imports, will be an alternative raw material for steel production, and this will create high value due to the usage of domestic resources. In this study, sponge iron production was tried to be optimized by using local sources. For this purpose, the effects of time, temperature and  $[C_{\text{Fix}}/Fe_{\text{Total}}]$  weight ratio on the Reduction Degree (%) of the important parameters effective in the production of sponge iron by using Divriği Iron Pellets and Dodurga Lignite as a reductant were studied using a Box-Wilson experimental design. The optimum parameters were determined as 82.59 min, 996.73 °C and 0.49, and the highest Reduction Degree (%) value was calculated as 96.46%. The sponge iron obtained with a 71.91% Reduction Degree contains 97.12% Fe, of which 7.12% is oxidized. It is evident that higher Fe contents may be attained with research carried out in optimum parameters.

**KEYWORDS:** Box-Wilson Experimental Design; Iron Pellets; Lignite; Optimization; Sponge Iron

Citation/Citar como: Sönmez, İ.; Şahbudak, K. (2023). "Optimization of sponge iron (direct reduced iron) production with Box-Wilson experimental design by using iron pellets and lignite as reductant". *Rev. Metal.* 59(2): e241. <https://doi.org/10.3989/revmetalm.241>

**RESUMEN:** *Optimización de la producción de hierro esponja (hierro de reducción directa) con diseño experimental Box-Wilson utilizando pellets de hierro y lignito como reductor.* Los minerales de hierro de Turquía pueden utilizarse para fabricar hierro esponja, y los recursos de carbón del país, abundantes a pesar de ser de mala calidad, pueden utilizarse como agente reductor. Con una producción de este tipo, el horno de arco eléctrico basado en la importación de chatarra, será una materia prima alternativa para la producción de acero, y esto creará un alto valor debido a la utilización de los recursos nacionales. En este estudio, se intentó optimizar la producción de hierro esponja utilizando fuentes locales. Para ello, se estudiaron los efectos del tiempo, la temperatura y la relación de peso  $[C_{\text{Fix}}/Fe_{\text{Total}}]$  sobre el Grado de Reducción (%) de los parámetros importantes que son eficaces en la producción de hierro esponja mediante el uso de Pellets de Hierro Divriği y Lignito Dodurga como reductor.

**Copyright:** © 2023 CSIC. This is an open-access article distributed under the terms of the Creative Commons Attribution 4.0 International (CC BY 4.0) License.

utilizando un diseño experimental Box-Wilson. Los parámetros óptimos determinados fueron: 82,59 min, 996,73 °C y 0,49, y el mayor valor de Grado de Reducción (%) se calculó como 96,46%. El hierro esponja obtenido con un Grado de Reducción del 71,91% contiene un 97,12% de Fe, del cual un 7,12% está oxidado. Es evidente que pueden alcanzarse contenidos de Fe más elevados con investigaciones realizadas con parámetros óptimos.

**PALABRAS CLAVE:** Diseño experimental Box-Wilson; Hierro esponja; Lignito; Optimización; Pellets de hierro

**ORCID ID:** İbrahim Sönmez (<https://orcid.org/0000-0001-8486-4663>); Kemal Şahbudak (<https://orcid.org/0000-0003-4853-6843>)

## 1. INTRODUCTION

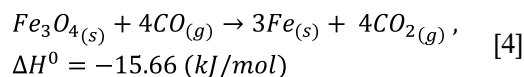
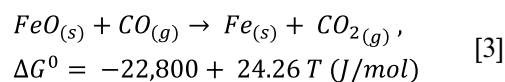
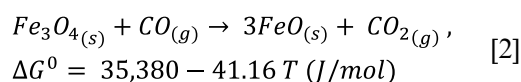
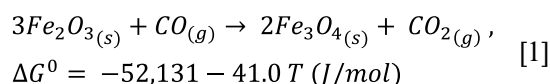
Oxidized iron-containing ore, concentrate, or pellets using solid or gas as a reducing agent without melting the metallic iron is obtained by the product is called sponge iron (Direct Reduced Iron, DRI). Sponge iron is utilized as an alternative raw material in electric arc furnaces and basic oxygen furnaces as charging materials because of its high degree of metallization, presence of certain oxide gangue, porous structure, stable composition, and low trace element content (Mazurov *et al.*, 1964; Leshchenko *et al.*, 1973; Selan *et al.*, 1996; Rose and Walden, 1988; Çamcı *et al.*, 2002; Chukwuleke *et al.*, 2009; Turgut, 2010; Kumar and Khana, 2012; Sen *et al.*, 2015; Dey *et al.*, 2015).

The majority of metals within the scope of metallurgy have been formed in oxides, sulfides, carbonates, silicates or complex compounds that form jointly. In addition to these natural raw materials, known as the primary metal source, secondary metal sources such as residues, slag, ash and flue dust, which had previously been physically, chemically or heat treated, have become increasingly important in this century, especially when ore grades are down (Khaki *et al.*, 2018). In addition, the production of sponge iron will continue to gain importance due to the decrease in the quantity and quality of coals suitable for coke production, increase in scrap prices, prolongation of scrap return time and difficulty in supply (Narçin and Aydın, 1991; Anameric and Kawatra, 2007; Zhang *et al.*, 2014; Khaki *et al.*, 2018).

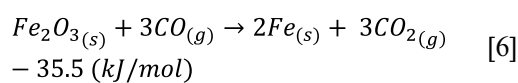
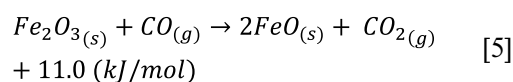
Depending on whether the reductant used is solid (C, coal) or gas (H<sub>2</sub>/CO), the production of sponge iron is divided into two categories (Komatina and Gudenau, 2004; Babich *et al.*, 2008; Çamcı *et al.*, 2002; Kumar and Khana, 2012; Chatterjee, 2012; Sen *et al.*, 2015). Compared to other reduction processes, the gas-based shaft furnace method has the advantages of high efficiency, low energy consumption, and low emission advantages. As a result, approximately 90% of the world's sponge iron production is done by gas-based direct reduction processes (Liu *et al.*, 2004; Chukwuleke *et al.*, 2009; Schenk, 2011; Guo *et al.*, 2016; WDRS, 2013; WDRS, 2015).

Numerous studies have been conducted on the direct reduction and kinetics of iron ore with coal. However, optimization of the DRI process requires detailed information on the thermal properties of

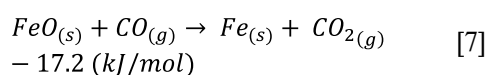
coal-ore mixtures and the basic mechanism of complex reduction reactions that are still not well understood (Liu *et al.*, 2004). The reactions occurring in the reduction of iron oxides with a CO-CO<sub>2</sub> mixture are given as follows in various sources [Reaction (1-10)] (Komatina and Gudenau, 2004; Liu *et al.*, 2004; Babich *et al.*, 2008; Chukwuleke *et al.*, 2009; Schenk, 2011; Guo *et al.*, 2016; Mombelli *et al.*, 2016; Chen *et al.*, 2017).



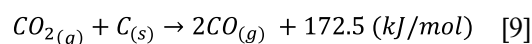
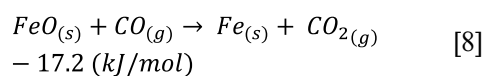
Indirect reduction below 1000 °C;

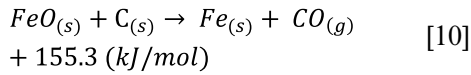


Indirect reduction in the range of 800-1000 °C;



Direct reduction with Boudouard reaction above 1000 °C;





Some studies have been carried out on sponge iron production using domestic resources in our country (Çamcı *et al.*, 2002; Geçim, 2006; Ersundu, 2007; Turgut, 2010; Dilmaç *et al.*, 2012). However, Dodurga Lignite has not been used in any previous studies. The aim of this study was to determine whether using Divriği Iron Pellets and Dodurga Lignite to produce sponge iron, and also to collect data on the evaluation of low quality domestic coals, which are now unappraisable with available equipment. For this purpose, the effects of temperature,  $[C_{Fix}/Fe_{Total}]$  weight ratio and time which are important parameters in sponge iron production on Reduction Degree (%) were investigated. By using Box-Wilson experiment, design and optimum parameters were determined.

## 2. MATERIALS AND METHODS

### 2.1. Material

In this study, iron pellets taken from Divriği with a diameter of 10-16 mm, using 0.8% bentonite as

a binder, sintered at 1250-1320 °C, with a compressive strength of 280 kg/pellet were used. The chemical analysis results of the iron pellets used in the experiments are given in Table 1. Also, Scanning Electron Microscopy (SEM) image analysis pictures are given in Fig. 1. The chemical analysis results of the lignite sample obtained from Dodurga Lignite Plant used as the reducing agent are given in Table 2. The coal sample was crushed and screened to the -11.20+4.75 mm particle size range.

The SEM images of the iron pellets in Fig. 1, show the hard agglomerates that have completed the grain formation. Solidified liquid phases are also at the junctions of coarse and fine grains.

Reduction experiments were carried out in a crucible with a lid using Protherm brand MoS-B 180/8 Model (1800 °C) Muffle Furnace without atmosphere control in Hitit University Faculty of Engineering Department of Metallurgical and Materials

TABLE 1. Average chemical analysis results of iron pellets

| Component                      | Weight (%) |
|--------------------------------|------------|
| Fe <sub>3</sub> O <sub>4</sub> | 45.00      |
| Fe <sub>2</sub> O <sub>3</sub> | 40.00      |
| FeO                            | 10.00      |
| MgO                            | 5.00       |

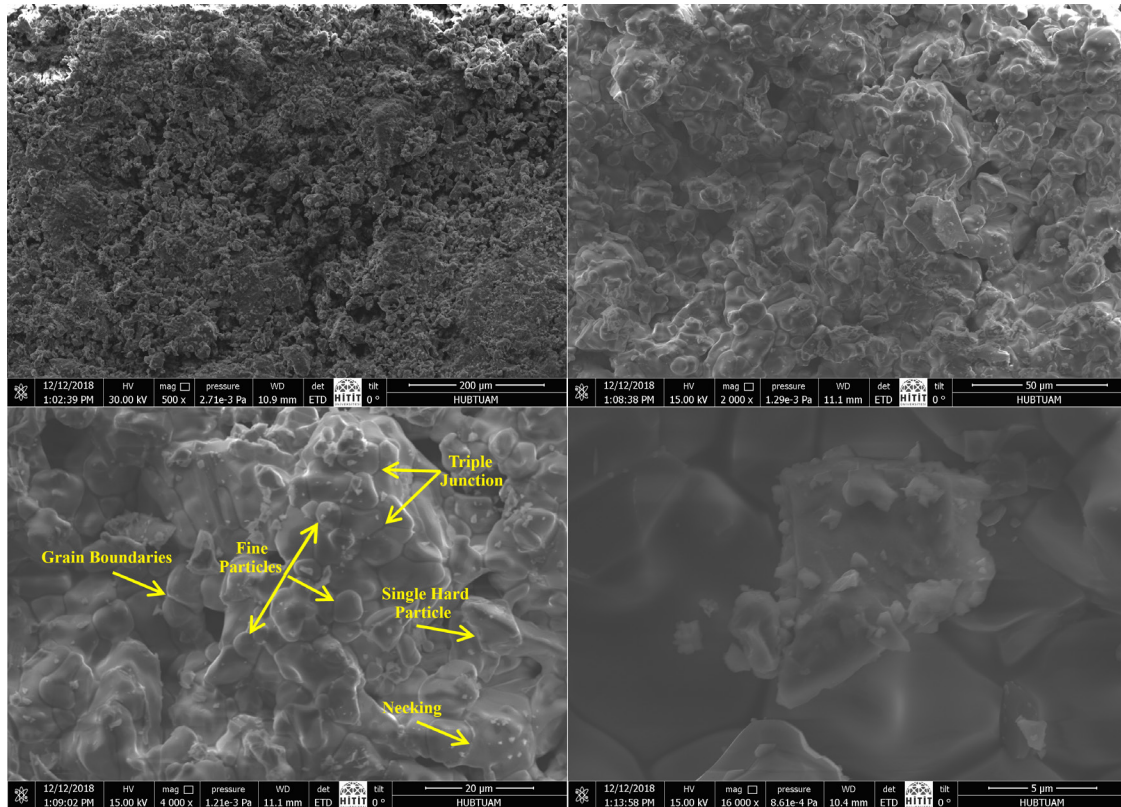


FIGURE 1. SEM image analysis of iron pellets.

TABLE 2. Coal analysis results

|                             | Types of analysis        | Original coal | Dry coal |
|-----------------------------|--------------------------|---------------|----------|
| Short Analysis              | Humidity (wt%)           | 13.48         | -        |
|                             | Ash (wt%)                | 9.55          | 11.4     |
|                             | Volatile Substance (wt%) | 44.25         | 51.4     |
|                             | Fixed Carbon (wt%)       | 32.72         | 37.2     |
|                             | TOTAL (wt%)              | 100           | 100      |
| Sulfurs                     | Burning Sulfur (wt%)     | 0.73          | 0.84     |
|                             | Sulfur in Ash (wt%)      | 0.10          | 0.12     |
|                             | Total Sulfur (wt%)       | 0.83          | 0.96     |
| Coking                      | Coke (wt%)               | 42.27         | 48.6     |
|                             | Gas (wt%)                | 57.73         | 51.4     |
| Thermal Values<br>(kcal/kg) | Lower Calories           | 4,361         | 5,132    |
|                             | Upper Calories           | 4,663         | 5,390    |

Engineering. Preheating was not used in the experiments, and the furnace heating and cooling were done at 20 °C·min<sup>-1</sup>. Scanning Electron Microscopy (SEM) image analysis of iron pellets and obtained sponge irons were carried out by using FEI brand Quanta 450 FEG model scanning electron microscope at Hitit University Scientific Technical Application and Research Center (HÜBTUAM). X-Ray Diffraction (XRD) analysis were carried out by using Rigaku brand DMAX IIIC model XRD Device in Cumhuriyet University Faculty of Engineering Department of Geological Engineering Laboratories.

## 2.2. Methods

Studies that calculate the reduction degree differently are found in the literature. Eq. (11) was used in the studies of Geçim (2006), Ersundu (2007), Schenk (2011), Chatterjee (2012), Khaki *et al.* (2018), and Eq. (12) was used in the studies of Babich *et al.* (2008), Lee *et al.* (2012), Chen *et al.* (2017), and Turgut (2010).

$$\text{Metallization Degree (\%)} = \frac{\text{Metallic Fe}}{\text{Total Fe}} * 100 \quad [11]$$

$$\text{Reduction Degree (\%)} = \frac{\text{Removing Oxygen}}{\text{Initial Oxygen}} * 100 \quad [12]$$

In this study; the Reduction Degree (%) values, which are a measure of how much of the total oxidized iron is reduced, were calculated using Eq. (13) given below.

$$\text{Reduction Degree (\%)} = \frac{\text{Amount of Reduced Oxide Iron in Sponge Iron}}{\text{Amount of Oxide iron in Feed Pellets}} * 100 \quad [13]$$

The reduction (sponge iron production) experiments carried out within the scope of the study by using Box-Wilson experimental design. Proper optimization was made for the parameters effective in the reduction. In this context, independent parameters in Box-Wilson experimental design method were used; time: 10-90 min, temperature: 900-1200 °C, and  $[C_{\text{Fix}}/Fe_{\text{Total}}]$  weight ratio: 0.40-0.50 (Hughes *et al.*, 1982; Lin *et al.*, 2003; Piotrowski *et al.*, 2005; Jozwiak *et al.*, 2007; Turgut, 2010).

## 2.3. Box-Wilson experimental design

The Box-Wilson statistical experimental design method includes three types of combinations. These are the axial (A), factorial (F), and center (C) points. The independent variables are at five levels, which are determined based on the number and range of variables in the experiment. The details of the method can be found elsewhere (Davies, 1956; Crozier, 1992).

Three operating parameters i.e., time, temperature and the  $[C_{\text{Fix}}/Fe_{\text{Total}}]$  weight ratio were chosen as the most important independent variables. The time ( $X_1$ ) was changed between 10 and 90 min, the temperature ( $X_2$ ) between 900 and 1200 °C and the  $[C_{\text{Fix}}/Fe_{\text{Total}}]$  weight ratio ( $X_3$ ) between 0.40 and 0.50. The experimental design consisted of six axial (A), eight factorial (F) and three center (C) points. The center point was repeated three times to estimate experimental error. The experimental conditions as coded values and real values used for the Box-Wilson statistical design are presented in Table 3.

The Reduction Degree (Y) was correlated with the other independent parameters ( $X_1, X_2, X_3$ ) using Eq. (14). Design Expert 8.0 computer program was

TABLE 3. Experimental conditions according to a Box-Wilson statistical design

| Experiment No. | Coded values   |                |                | Real values |                  |   |
|----------------|----------------|----------------|----------------|-------------|------------------|---|
|                | X <sub>1</sub> | X <sub>2</sub> | X <sub>3</sub> | Time (min)  | Temperature (°C) | [C <sub>Fix</sub> /Fe <sub>Total</sub> ] weight ratio |
| A1             | 1.73           | 0              | 0              | 90          | 1,050            | 0.45  |
| A2             | -1.73          | 0              | 0              | 10          | 1,050            | 0.45  |
| A3             | 0              | 1.73           | 0              | 50          | 1,200            | 0.45  |
| A4             | 0              | -1.73          | 0              | 50          | 900              | 0.45  |
| A5             | 0              | 0              | 1.73           | 50          | 1,050            | 0.50  |
| A6             | 0              | 0              | -1.73          | 50          | 1,050            | 0.40  |
| F1             | 1              | 1              | 1              | 73.09       | 1,136.6          | 0.48  |
| F2             | 1              | 1              | -1             | 73.09       | 1,136.6          | 0.42  |
| F3             | 1              | -1             | 1              | 73.09       | 963.4            | 0.48  |
| F4             | 1              | -1             | -1             | 73.09       | 963.4            | 0.42  |
| F5             | -1             | 1              | 1              | 26.91       | 1,136.6          | 0.48  |
| F6             | -1             | 1              | -1             | 26.91       | 1,136.6          | 0.42  |
| F7             | -1             | -1             | 1              | 26.91       | 963.4            | 0.48  |
| F8             | -1             | -1             | -1             | 26.91       | 963.4            | 0.42  |
| C1             | 0              | 0              | 0              | 50          | 1,050            | 0.45  |
| C2             | 0              | 0              | 0              | 50          | 1,050            | 0.45  |
| C3             | 0              | 0              | 0              | 50          | 1,050            | 0.45  |
| C (Ave.)       | 0              | 0              | 0              | 50          | 1,050            | 0.45  |

used for the determination of the coefficients of Eq. (14) by regression analysis of the experimental data.

$$\begin{aligned}
 Y = & -13,971.17 + 498.46(X_1) + 25.86(X_2) + \\
 & 2,322.84(X_3) - 0.90(X_1 * X_2) - \\
 & 143.68(X_1 * X_3) - 3.60(X_2 * X_3) - 4.14(X_1 * X_1) - \\
 & 0.012(X_2 * X_2) + 2,693.33(X_3 * X_3) + \\
 & 0.09(X_1 * X_2 * X_3) + 0.007743(X_1 * X_1 * X_2) + \\
 & 0.53(X_1 * X_1 * X_3) + 0.0004208(X_1 * X_2 * X_2) - \\
 & 0.000003832(X_1 * X_1 * X_2 * X_2)
 \end{aligned}
 \tag{14}$$

### 3. RESULTS AND DISCUSSION

A comparison of the experimental and predicted values for the Reduction Degree (%) is summarized in Table 4. The observed Reduction Degree (%) varied between 28.32% and 72.12%. The determination coefficient (R<sup>2</sup> values) between the observed and predicted values was 0.9996 for Reduction Degree (%), indicating a good correlation between the observed and predicted values.

#### 3.1. The effect of time and temperature

Variation of the Reduction Degree (%) in a constant [C<sub>Fix</sub>/Fe<sub>Total</sub>: 0.45] weight ratio depending on time and temperature is given in Fig. 2. In addition,

TABLE 4. Observed and predicted Reduction Degree (%) values

| Experiment No. | Reduction Degree (%) |           |
|----------------|----------------------|-----------|
|                | Observed             | Predicted |
| A1             | 72.12                | 72.12     |
| A2             | 67.47                | 67.47     |
| A3             | 71.91                | 71.91     |
| A4             | 34.21                | 34.21     |
| A5             | 66.31                | 66.31     |
| A6             | 68.31                | 68.31     |
| F1             | 68.36                | 69.33     |
| F2             | 28.32                | 27.73     |
| F3             | 67.60                | 67.94     |
| F4             | 59.38                | 59.40     |
| F5             | 41.80                | 42.00     |
| F6             | 41.10                | 41.28     |
| F7             | 44.82                | 45.23     |
| F8             | 33.10                | 33.06     |
| C (Ave.)       | 60.58                | 60.58     |

SEM image analysis of sponge iron obtained from Experiment No.: C [Center] and Experiment No.: A1 is given in Fig. 3 and Fig. 4, respectively.

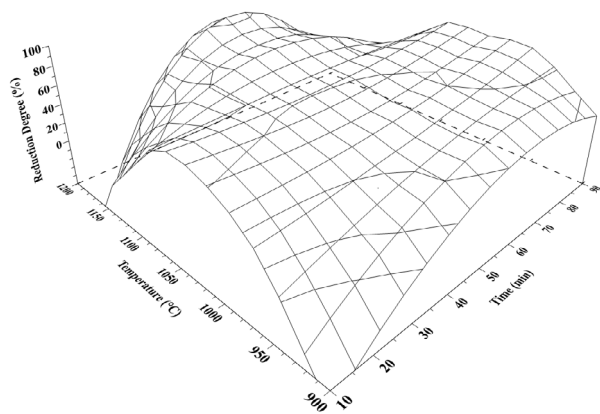


FIGURE 2. Effect of time and temperature on Reduction Degree (%) [ $C_{Fix}/Fe_{Total}$ : 0.45].

As it can be seen from Fig. 2, as the temperature rises up to 1,000 °C, the Reduction Degree (%) rose steadily during the course of around 80 minutes. Especially at temperatures below 950 °C, the maximum Reduction Degree (%) values reached in 80 minutes started to decrease again with increasing time. The Reduction Degree (%) values in the temperature range 1000-1050 °C did not change much

depending on the time. However, the Reduction Degree (%) values decreased rapidly both at low (less than 40 min) and high (over 60 min) times, especially at temperatures above 1100 °C. The Reduction Degree (%) reached its maximum value in about 50 min in this temperature range.

The basic principles of chemical thermodynamics and kinetics and the basic laws of diffusion predict that an increase in the reduction temperature or prolonged reaction time at low temperatures can improve the degree of reduction of iron oxide (El-Geassy, 1986; Pawlik *et al.*, 2007). The temperature greatly affects the Reduction Degree (%). Since the main reduction reactions [reduction of magnetite to wustite] are endothermic and facilitated by high temperature, the Reduction Degree (%) increases with increasing temperature. Thus, an increase in temperature caused an increase in diffusion and reduction rates. This is described by Liu *et al.* (2004), Wang *et al.* (2012), Yi *et al.* (2012), Zhang *et al.* (2014), Guo *et al.* (2016), and Chen *et al.* (2017). The reduction reaction in the CO atmosphere [reduction of magnetite and wustite to iron] is exothermic, so dynamic conditions develop simultaneously, although thermodynamic conditions deteriorate with rising temperature (Wang *et al.*, 2012). The increase in the Reduction Degree (%) with increasing time can be attributed to a large contact area between the

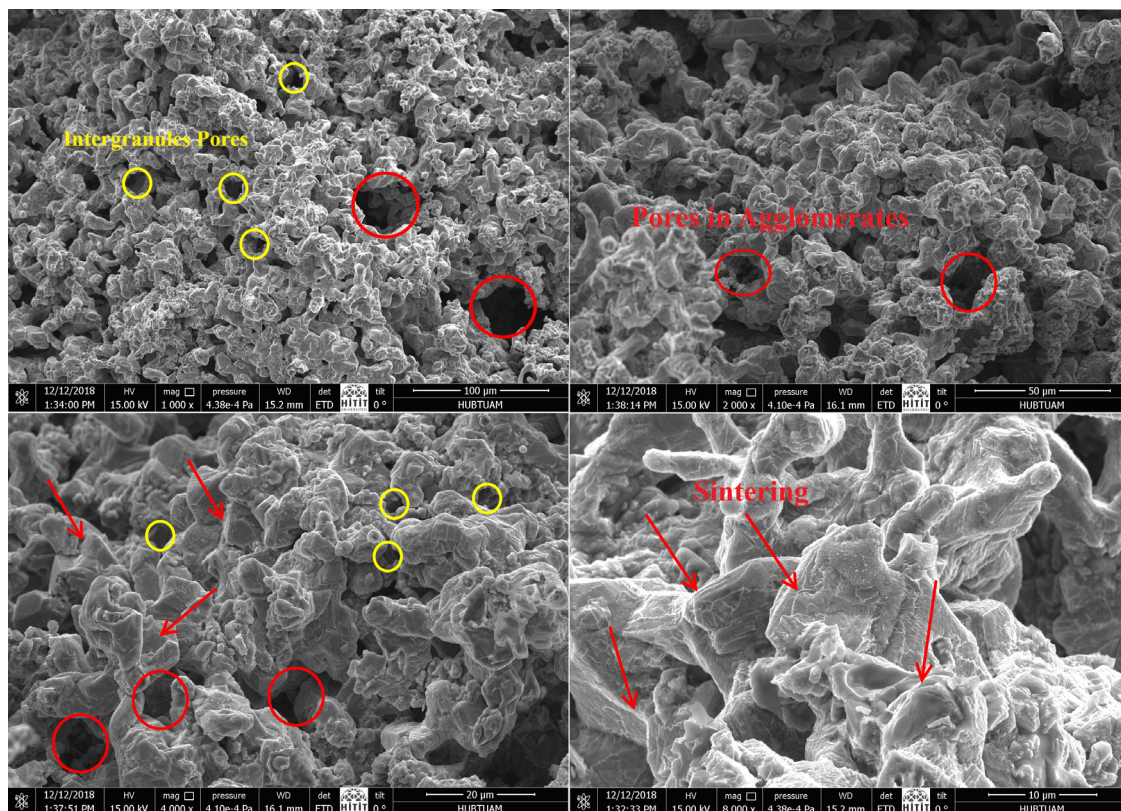


FIGURE 3. SEM image analysis of the obtained sponge iron [Experiment No.: C].

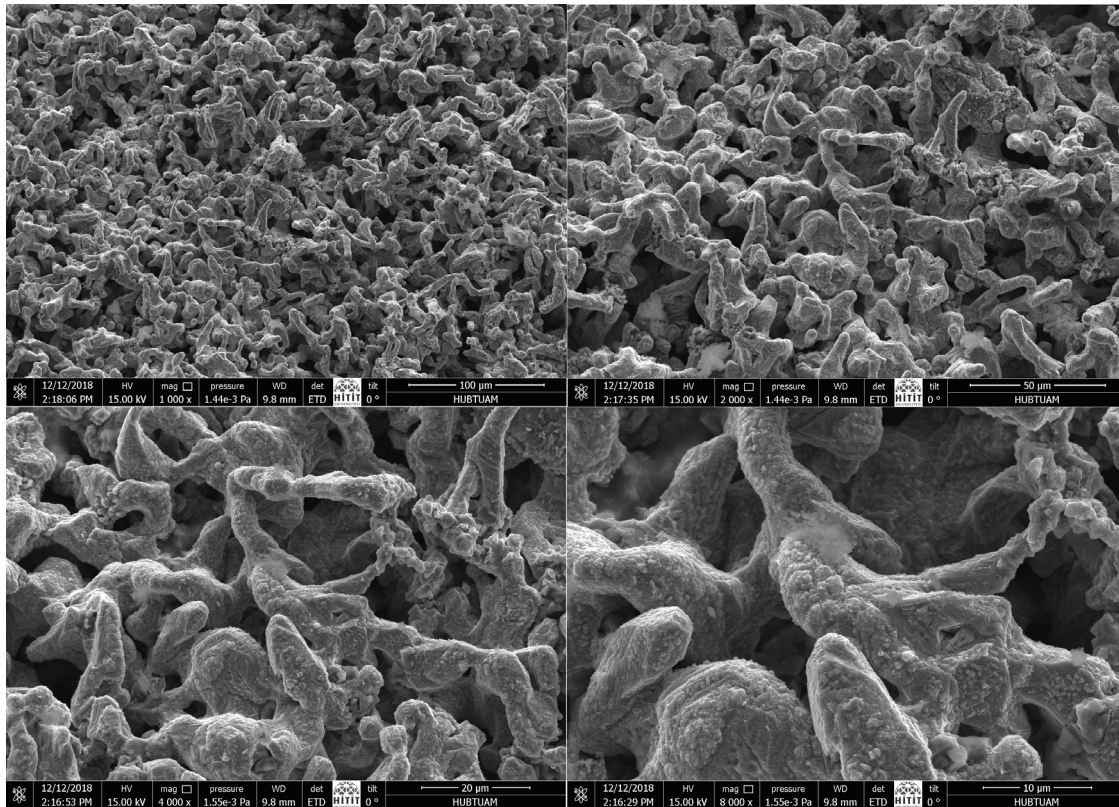


FIGURE 4. SEM image analysis of the obtained sponge iron [Experiment No.: A1].

reducing gas and the pellets. The samples produced in this study were pellets with an approximate porosity of 60%, giving rise to the contact of gas with more grains of iron oxide. The reducing gas readily reacted by diffusing into the pellets and the gases formed from the reactions were easily removed from the pellets. The reduction in the rate of increase of the Reduction Degree (%) as the time increases further can be attributed to the coating of the outer surface of the pellets with an iron “shell” and the reduction of penetration of the reducing gas into the pellets as the reactions progress. Simultaneously, it is difficult for the gases formed as a result of reactions to escape out of the pellets. Additionally, unreacted pellet cores were continuously reduced. After 70 min, the increase in the Reduction Degree (%) slowed down and reached a constant level over longer periods. This shows that the reduction reactions are almost completed, and a large proportion of  $\text{Fe}_2\text{O}_3$ s are reduced to Fe. These results are consistent with the results of Guo *et al.* (2016).

The SEM image analysis of the sponge iron obtained in Experiment No.: C given in Fig. 3 shows that the sponge structure, which is highly reduced and clinging to the neck regions with the effect of temperature, can be seen. The structure is completely sintered and does not contain a different phase at the grain boundaries. It is seen that pore sizes

are between 20-50  $\mu\text{m}$  in agglomerates, as seen by big red circles, and intergranular pores are between 1-10  $\mu\text{m}$  as illustrated by small yellow circles. It is observed that the round-edged particles close to the sphere are reduced and topo chemically  $\text{FeO}$  to Fe structures. The growth morphology of Fe in the body-centered cubic or face-centered cubic cage in the cubic crystal, as seen by big red circles and the presence of a small amount of  $\text{Fe}_2\text{O}_3$  or  $\text{FeO}$  structure, were also determined by fractures. These features are indicated by arrows caused by sharp crack propagation, as seen by small yellow circles between sinter grains. It is readily apparent the sintering and neck formation of reduced metal-like structures both in deformed form and as sharp ceramic cleavage fractures. Regional hard agglomerates have been identified, where fine-grained Fe structures reduced from coarse-grained Fe-O structures are the driving force for sintering by liquidifying surface metals which are shown as long bridge-like metallic horns or deformed buckled pieces.

It is seen in Fig. 4 that the SEM image analysis of the sponge iron obtained in Experiment No.: A1 consists of sponge iron structures of metal character that are thought to contain mostly Fe, similar to the SEM image analysis of sponge iron obtained by Experiment No.: C illustrated in Fig. 3. It has a more homogeneously distributed pore size, and the aver-

age pore size, is identical across the entire structure in the range of 2-10 µm.

### 3.2. Effect of Time and $[C_{Fix}/Fe_{Total}]$ Weight Ratio

The variation of the Reduction Degree at a constant temperature of 1050 °C, depending on the time and  $[C_{Fix}/Fe_{Total}]$  weight ratio, is given in Fig. 5. Also, SEM image analysis of sponge iron obtained from Experiment No.: A5 is given in Fig. 6.

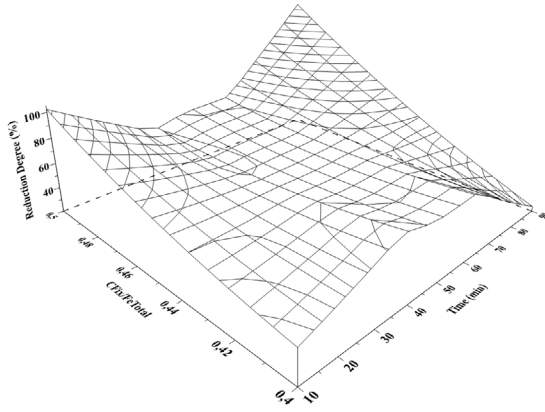


FIGURE 5. Effect of time and  $[C_{Fix}/Fe_{Total}]$  weight ratio on the Reduction Degree (%) (Temperature: 1050 °C).

Figure 5 shows that with the increase in time, the Reduction Degree (%) increases and reaches its maximum values in the 40-60 min range. At higher times, the Reduction Degree (%) again decreased. In the 0.44-0.46  $[C_{Fix}/Fe_{Total}]$  weight ratio range, the Reduction Degree (%) did not change much depending on the time. Time's effect caused the Reduction Degree (%) values to drop precipitously to their lowest points in terms of the higher value of  $[C_{Fix}/Fe_{Total}]$  between 40 and 60 min, then rise precipitously to their highest points again after 60 min. The highest Reduction Degree (%) values were reached at the maximum time values and  $[C_{Fix}/Fe_{Total}]$  weight ratio. In other words; The Reduction Degree (%) values increased due to the increase of the  $[C_{Fix}/Fe_{Total}]$  weight ratio in low and high times, whereas the Reduction Degree (%) decreased as the  $[C_{Fix}/Fe_{Total}]$  weight ratio increased in the medium periods (in the range of 40-60 min).

It is seen that the sponge iron obtained with Experiment No.: A5 has a grain size as in SEM image analysis of the sponge iron obtained with Experiment No.: C illustrated in Fig. 3 and Experiment No.: A3 illustrated in Fig. 8, and due to the similarity of the reductant, the particles are partially attached to each other, and the sintered structure is developed. The stratified growth pattern is similar

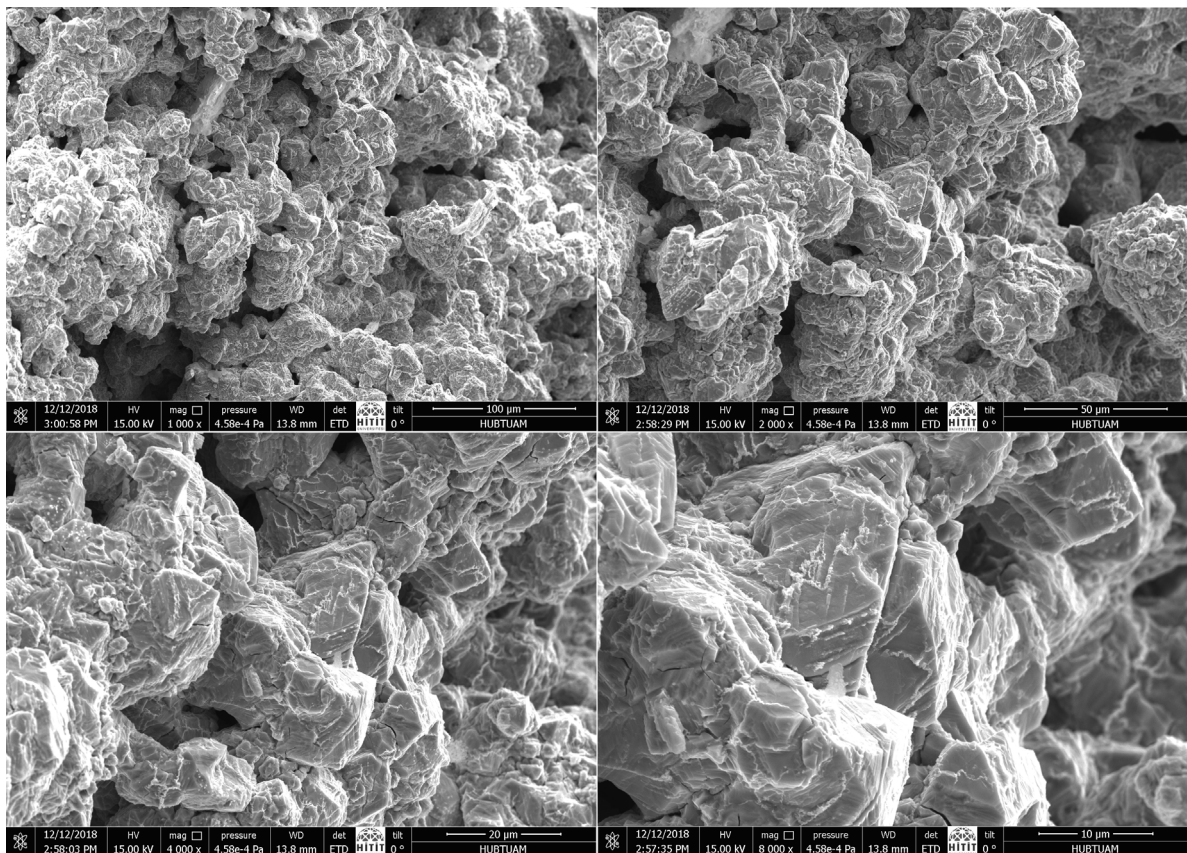


FIGURE 6. SEM image analysis of the obtained sponge iron [Experiment No.: A5].

to the body-centered cubic or face-centered cubic growth morphology of Fe. The amount of oxide is also understood from the electron charge. As it is very well known, since the electron charge takes place on the edges of ceramic-like materials even if it was gold-coated, the higher the amount of Fe<sub>2</sub>O<sub>3</sub> or FeO, the lighter the image. The sharp edges are also an indication of oxide formation due to high stratigraphy of grown material. As it is seen from previous SEM images, the reduced Fe is elongated and deformed bars.

### 3.3. Effect of [C<sub>Fix</sub>/Fe<sub>Total</sub>] Weight Ratio and Temperature

The change in the Reduction Degree (%) depending on [C<sub>Fix</sub>/Fe<sub>Total</sub>] weight ratio and temperature at 50 min fixed time is given in Fig. 7. In addition, SEM image analysis of sponge iron obtained from Experiment No.: A3 is given in Fig. 8.

As it can be seen from Fig. 7; at temperatures below about 1050 °C, the Reduction Degree (%) values tend to decrease due to the increase in the [C<sub>Fix</sub>/Fe<sub>Total</sub>] weight ratio. The Reduction Degree (%) values did not change much due to the increase in [C<sub>Fix</sub>/Fe<sub>Total</sub>] weight ratio at the temperatures above this value, but the maximum Reduction Degree (%) was reached at the highest temperature and [C<sub>Fix</sub>/Fe<sub>Total</sub>]

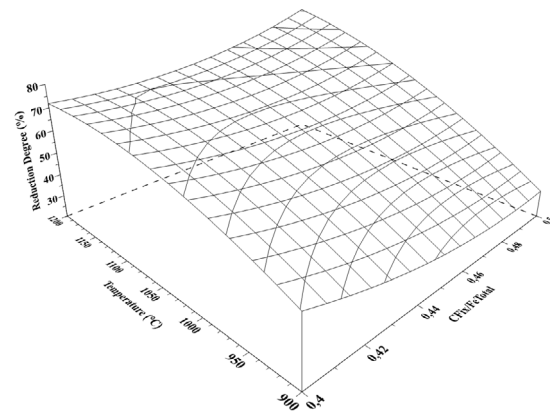


FIGURE 7. The effect of [C<sub>Fix</sub>/Fe<sub>Total</sub>] weight ratio and temperature on the Reduction Degree (%) (Time: 50 min).

weight ratio values. In other words, the Reduction Degree (%) values increased due to the increase in temperature. This increase in the Reduction Degree (%) values was faster up to a temperature of about 1050 °C, especially at high [C<sub>Fix</sub>/Fe<sub>Total</sub>] weight ratio values. The rate of increase of the Reduction Degree (%) values decreased due to the temperature increase above about 1050 °C.

The increase in the Reduction Degree (%) due to the increase in temperature is consistent with the

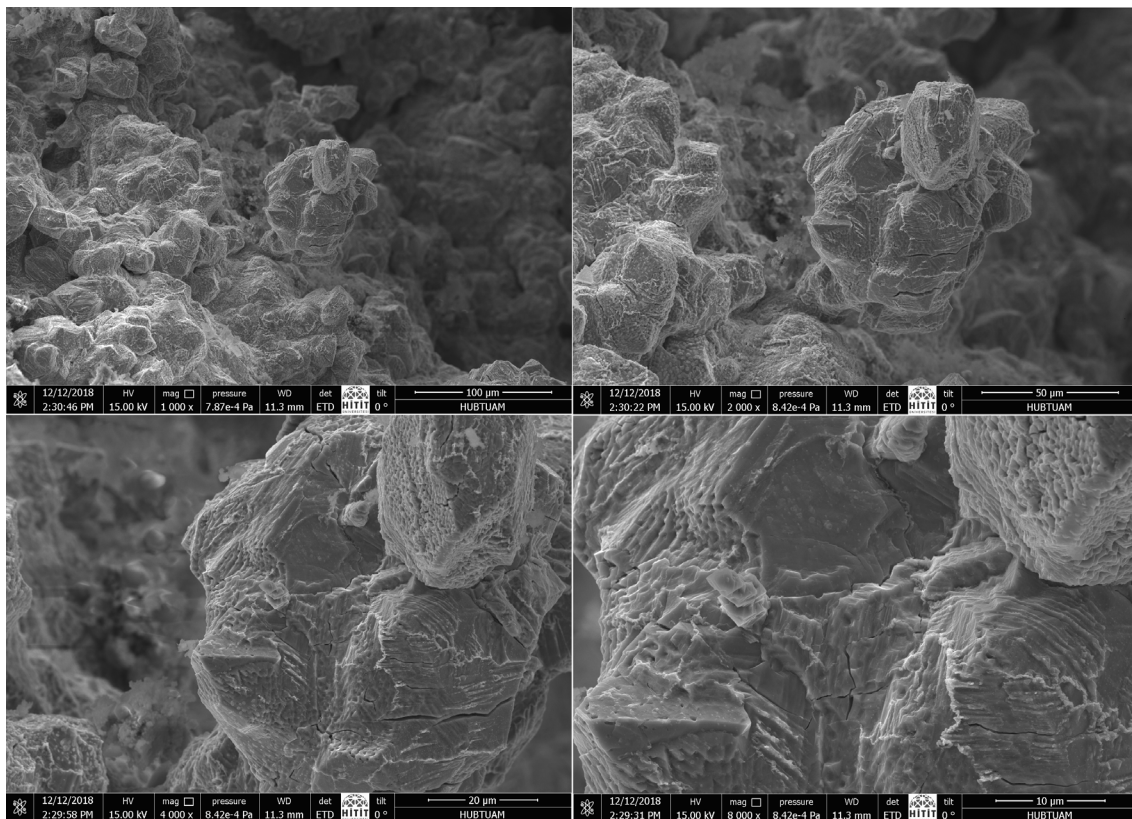


FIGURE 8. SEM image analysis of the obtained sponge iron [Experiment No.: A3].

results obtained by Ersundu (2007) and Lee *et al.* (2012). Furthermore, it can be said that the effect of  $[C_{\text{Fix}}/Fe_{\text{Total}}]$  weight ratio on the Reduction Degree (%) at constant temperature and time remains weak among other parameters. Similar results are expressed by Ersundu (2007) and Khaki *et al.* (2018).

In Fig. 8, Fe-grains reduced by topochemical reaction and fast-growing fully concentrated sinter structure can be seen. Sintering may have occurred during the Fe reduction process, since the resulting hard agglomerates had a compact structure devoid of pores. This procedure continues up to all surfaces are grown in the certain directions of maximum packing density and again produces surface oxides. Fe crystals grow towards the surface as a result of a reduction that develops from the outside to the inside. During this process, the crystals encounter surface oxides and are reduced once more. The most important proof of this situation is the brittle crack advances on the surface. In certain regions, the crack is stopped, which can be thought to be due to the energy absorption of the metallized regions.

### 3.4. Optimization

The sponge iron obtained by Experiment No.: A3 with a Reduction Degree (%) of 71.91% contains a total of 97.12% Fe, of which 7.12% is oxidized. Optimum time ( $X_1$ ; 10-90 min), temperature ( $X_2$ ; 900-1200 °C), and  $[C_{\text{Fix}}/Fe_{\text{Total}}]$  weight ratio ( $X_3$ ; 0.40-0.50) provided that selected parameters are the most important independent variables in the production of sponge iron, respectively, 82.59 min, 996.73 °C and 0.49 were determined, and the highest Reduction Degree (%) value was calculated as 96.46%.

## 4. CONCLUSIONS

- The Box-Wilson statistical experimental design procedure was found to be applicable to modeling the effects of important variables on the Reduction Degree (%) of iron ore pellets. The regression analysis's predicted response functions were consistent with the experiments' findings.
- The effects of time, temperature, and  $[C_{\text{Fix}}/Fe_{\text{Total}}]$  weight ratio on the Reduction Degree (%), which are among the most important parameters effective in sponge iron production, were investigated and the optimum parameters were determined as 82.59 min, 996.73 °C and 0.49, respectively, and the highest Reduction Degree (%) value was calculated as 96.46%.
- The sponge iron obtained with 71.91% Reduction Degree (%) contains a total of 97.12% Fe, of which 7.12% is oxidized. It is seen that higher Fe contents can be achieved with a study to be performed in optimum parameters.
- The sponge iron thus obtained may be an alternative to pig iron in steel production. This study

determined the suitability of domestic resources such as Divriği Iron Pellets and Dodurga Lignite for sponge iron production, and data related to the evaluation of low-quality domestic coals were produced. However, additional research is needed to determine, based on complicated reaction processes and transformation reactions of other compounds, whether or not low-quality iron ores and other coal sources in our nation are suitable for the manufacture of sponge iron. In addition, undesirable impurities such as S, Si, and P in steel production should be examined in detail and controlled in sponge iron production.

## ACKNOWLEDGMENTS

This work was supported by the Hitit University Scientific Research Project Coordination Unit (grant number MUH19001.17.004).

## REFERENCES

- Anameric, B., Kawatra, S.K. (2007). Properties and features of direct reduced iron. *Miner. Process. Extr. Metall. Rev.* 28 (1), 59–116. <https://doi.org/10.1080/08827500600835576>.
- Babich, A., Senk, D., Gudenau, H.W., Mavrommatis, K.T. (2008). *Ironmaking*. RWTH Aachen University, Department of Ferrous Metallurgy, Aachen, Germany.
- Çamcı, L., Aydın, S., Arslan, C. (2002). Reduction of iron oxides in solid wastes generated by steelworks. *Turkish J. Eng. Env. Sci.* 26, 37–44. <https://aj.tubitak.gov.tr/engineering/issues/muh-02-26-1/muh-26-1-5-0012-2.pdf>.
- Chatterjee, A. (2012). *Sponge Iron Production by Direct Reduction of Iron Oxide*. 2nd ed., PHI Learning Private Limited, Delhi, India.
- Chen, H., Zheng, Z., Chen, Z., Bi, X.T. (2017). Reduction of hematite ( $Fe_2O_3$ ) to metallic iron (Fe) by CO in a micro fluidized bed reaction analyzer: A multistep kinetics study. *Powder Technol.* 316, 410–420. <https://doi.org/10.1016/j.powtec.2017.02.067>.
- Chukwuleke, O.P., Cai, J.J., Chukwujekwu, S., Xiao S. (2009). Shift from coke to coal using direct reduction method and challenges. *J. Iron Steel Res. Int.* 16 (2), 1–5. [https://doi.org/10.1016/s1006-706x\(09\)60018-2](https://doi.org/10.1016/s1006-706x(09)60018-2).
- Crozier, R.D. (1992). *Flotation*. Pergamon Press.
- Davies, O.L. (1956). *The Design and Analysis of Industrial Experiments*. Hafner Publishing Co., New York.
- Dey, N.R., Prasad, A.K., Singh, S.K. (2015). Energy survey of the coal based sponge iron industry. *Case Stud. Therm. Eng.* 6, 1–15. <https://doi.org/10.1016/j.csite.2015.04.001>.
- Dilmaç, N., Yörük, S., Gülaboğlu, Ş.M. (2012). Determination of reduction degree of direct reduced iron via FT-IR spectroscopy. *Vib. Spectrosc.* 61, 25–29. <https://doi.org/10.1016/j.vibspec.2012.03.008>.
- El-Geassy, A.A. (1986). Gaseous reduction of  $Fe_2O_3$  compacts at 600 to 1050 °C. *J. Mater. Sci.* 21 (11), 3889–3900. [https://doi.org/10.1016/0168-7336\(87\)80032-3](https://doi.org/10.1016/0168-7336(87)80032-3).
- Ersundu, A.E. (2007). *The suitability investigation of domestic iron ores for sponge iron production*. Istanbul Technical University, Graduate School of Natural and Applied Sciences, Istanbul, Turkey.
- Geçim, M.K. (2006). *The investigation of sponge iron production parameters by using iron oxide pellets with domestic lignite coal*. Istanbul Technical University, Graduate School of Natural and Applied Sciences, Istanbul, Turkey.
- Guo, D., Zhu, L., Guo, S., Cui, B., Luo, S., Laghari, M., Chen, Z., Ma, C., Zhou, Y., Chen, J., Xiao, B., Hu, M., Luo, S. (2016). Direct reduction of oxidized iron ore pellets using biomass syngas as the reducer. *Fuel Processing Technology* 148, 276–281. <https://doi.org/10.1016/j.fuproc.2016.03.009>.

- Hughes, R., Kam, E.K.T., Mogadam-Zadeh, H. (1982). The reduction of iron ores by hydrogen and carbon monoxide and their mixtures. *Thermochim. Acta* 59 (3), 361–377. [https://doi.org/10.1016/0040-6031\(82\)87158-x](https://doi.org/10.1016/0040-6031(82)87158-x).
- Jozwiak, W.K., Kaczmarek, E., Maniecki, T.P., Ignaczak, W., Maniukiewicz, W. (2007). Reduction behavior of iron oxides in hydrogen and carbon monoxide atmospheres. *Appl. Catal. A-Gen.* 326 (1), 17–27. <https://doi.org/10.1016/j.apcata.2007.03.021>.
- Khaki, J.V., Shalchian, H., Rafsanjani-Abbasi, A., Alavifard, N. (2018). Recovery of iron from a high-sulfur and low-grade iron ore. *Thermochim. Acta* 662, 47–54. <https://doi.org/10.1016/j.tca.2018.02.010>.
- Komatina, M., Gudenau, H.W. (2004). The sticking problem during direct reduction of fine iron ore in the fluidized bed. *Metalurgija – J. Metall.* 10 (4), 309–328. <https://doi.org/10.30544/378>.
- Kumar, V., Khana, S. (2012). Recovery and utilization of waste heat in a coal based sponge iron process. *Chem. Eng. Process.* 56, 19–28. <https://doi.org/10.1016/j.ccep.2012.03.002>.
- Lee, Y.S., Ri, D.W., Yi, S.H., Sohn, I. (2012). Relationship between the reduction degree and strength of DRI pellets produced from iron and carbon bearing wastes using an RHF simulator. *ISIJ Int.* 52 (8), 1454–1462. <https://doi.org/10.2355/isijinternational.52.1454>.
- Leshchenko, I.P., Tereshchenko, V.T., Martynov, O.V., Trakhimovich, V.I., Borzenkov, D.V. (1973). The use of sponge iron in steel smelting. *Metallurgist* 17 (7), 491–494. <https://doi.org/10.1007/bf01094155>.
- Lin, H.Y., Chen, Y.W., Li, C. (2003). The mechanism of reduction of iron oxide by hydrogen. *Thermochimica Acta* 400 (1–2), 61–67. [https://doi.org/10.1016/s0040-6031\(02\)00478-1](https://doi.org/10.1016/s0040-6031(02)00478-1).
- Liu, G., Strezov, V., Lucas, J.A., Wibberley, L.J. (2004). Thermal investigations of direct iron ore reduction with coal. *Thermochim. Acta* 410, 133–140. [https://doi.org/10.1016/s0040-6031\(03\)00398-8](https://doi.org/10.1016/s0040-6031(03)00398-8).
- Mazurov, E.F., Gnuchev, S.M., Skripchuk, V.S., Markin, A.A., Lyalin, E.S. (1964). Sponge iron as a charge material. *Metallurgist* 8 (11), 602–604. <https://doi.org/10.1007/bf01133796>.
- Mombelli, D., Cecca, C.D., Mapelli, C., Barella, S., Bondi, E. (2016). Experimental analysis on the use of BF-sludge for the reduction of BOF-powders to direct reduced iron (DRI) production. *Process Saf. Environ. Prot.* 102, 410–420. <https://doi.org/10.1016/j.psep.2016.04.017>.
- Narçin, N., Aydın, S. (1991). Sponge iron and its use in electric arc furnaces. *Metalurji, Chamber of Metallurgical and Materials Engineers of Turkey Publication* 77, 28–32.
- Pawlik, C., Schuster, S., Eder, N., Winter, F., Mali, H., Fischer, H., Schenk, J.L. (2007). Reduction of iron ore fines with CO-rich gases under pressurized fluidized bed conditions. *ISIJ Int.* 47 (2), 217–225. <https://doi.org/10.2355/isijinternational.47.217>.
- Piotrowski, K., Mondal, K., Lorethova, H., Stonawski, L., Szymański, T., Wiltowski, T. (2005). Effect of gas composition on the kinetics of iron oxide reduction in a hydrogen production process. *Int. J. Hydrog. Energy* 30 (15), 1543–1554. <https://doi.org/10.1016/j.ijhydene.2004.10.013>.
- Rose, F., Walden, H. (1988). Midrex and SL/RN direct reduction. *Proven. Alternatives for Steelmaking* 1–4.
- Schenk, J.L. (2011). Recent status of fluidized bed technologies for producing iron input materials for steelmaking. *Particuology* 9 (1), 14–23. <https://doi.org/10.1016/j.partic.2010.08.011>.
- Selan, M., Lehrhofer, J., Friedrich, K., Kordes, K., Simader, G. (1996). Sponge iron: Economic, ecological, technical and process-specific aspects. *J. Power Sources* 61 (1–2), 247–253. [https://doi.org/10.1016/s0378-7753\(96\)02366-x](https://doi.org/10.1016/s0378-7753(96)02366-x).
- Sen, R., Dehiya, S., Pandel, U., Banerjee, M.K. (2015). Utilization of low grade coal for direct reduction of mill scale to obtain sponge iron: Effect of reduction time and particle size. *Procedia Earth Planet. Sci.* 11, 8–14. <https://doi.org/10.1016/j.proeps.2015.06.003>.
- Turgut, E. (2010). *Production of sponge iron by direct reduction*. MSc thesis, Kocaeli University, Graduate School of Natural and Applied Sciences, Kocaeli, Turkey.
- Wang, Z., Chu, M., Liu, Z., Chen, S., Xue, X. (2012). Effects of temperature and atmosphere on pellets reduction swelling index. *J. Iron Steel Res. Int.* 19 (10), 7–12. [https://doi.org/10.1016/s1006-706x\(12\)60144-7](https://doi.org/10.1016/s1006-706x(12)60144-7).
- WDRS (2013). World Direct Reduction Statistics. <https://dokumen.tips/documents/world-direct-reduction-statistics-2013.html> [accessed June 2023].
- WDRS (2015). World Direct Reduction Statistics. <https://felezatkharvarmianeh.ir/Panel/%20Attachments/636034999812317158.pdf>. <https://middleeastmetals.ir> [accessed June 2023].
- Yi, Ly., Huang, Zc., Peng, H., Jiang, T. (2012). Action rules of H<sub>2</sub> and CO in gas-based direct reduction of iron ore pellets. *J. Cent. South Univ.* 19, 2291–2296. <https://doi.org/10.1007/s11771-012-1274-0>.
- Zhang, T., Lei, C., Zhu, Q. (2014). Reduction of fine iron ore via a two-step fluidized bed direct reduction process. *Powder Technol.* 254, 1–11. <https://doi.org/10.1016/j.powtec.2014.01.004>.